

NUMERICAL STUDY OF TEMPERATURE TRANSPORT IN HOMOGENEOUS ISOTROPIC TURBULENCE

A. Couzinet^{†,*}, B. Bédard[†], O. Simonin[†]

[†]Institut de Mécanique des Fluides de Toulouse, UMR 5502 CNRS/INPT/UPS,
Allée du Pr. Camille Soula, 31400 Toulouse, France.

*Email: couzinet@imft.fr

ABSTRACT

This paper presents DNS results on heat transport in homogeneous isotropic turbulence. This study is focussing on the Lagrangian fluid turbulence statistics (Lagrangian correlations functions) which are crucial for the analysis and the modeling of the fluid turbulent properties along discrete particle trajectories. Finally, a velocity-scalar Lagrangian stochastic approach is proposed and evaluated from the DNS results.

INTRODUCTION

With the increasing development of computing facilities, Direct Numerical Simulation has given a boost to describe complex phenomena in turbulent flows. Simulations of particle dispersion and mixing of a passive scalar [5] in isotropic homogeneous turbulence have been successfully investigated since over 15 years. Nevertheless, heat transport in turbulent two-phase flows have been less addressed. Preliminary stages of a study aiming to the development of heat transport modeling in particle-laden turbulent flows [1] are presented.

First, velocity and temperature Eulerian fields are fully predicted using DNS. Then, numerous fluid particle trajectories are computed to obtain Lagrangian informations (velocity and temperature Lagrangian autocorrelation and cross-correlation functions). At last, these correlation functions are compared with the ones derived from given stochastic models.

PROBLEM FORMULATION

Numerical approach

The Direct Numerical Simulation flow conditions correspond to a stationary isotropic homogeneous turbulent flow which is sustained by applying a stochastic forcing scheme proposed by Eswaran and Pope [2] and used by Fevrier et al. [3]. The parameters of stationary homogeneous isotropic turbulence are reported on Tab. 1 : fluid is air, Re_L is the Reynolds number based on the integral scale.

Following [4], the temperature fluctuation transport equation (1) is written assuming a mean given temperature gradient $\frac{\partial \langle \theta_f \rangle}{\partial x_2} = \gamma$ in the v_f -direction (with $v_f = u_{f_2}$),

$$\frac{\partial \theta'_f}{\partial t} + u'_{f_j} \frac{\partial \theta'_f}{\partial x_j} = v'_f \gamma + \kappa_f \frac{\partial^2 \theta'_f}{\partial x_j \partial x_j} \quad (1)$$

With $\kappa_f = \frac{\lambda_f}{\rho_f C_{p_f}}$ the thermal diffusivity of fluid. The boundary conditions for velocity and tem-

perature fluctuations are periodic in the three directions. The Navier-Stokes and temperature equations are integrated in space, using a finite-volume method with a second order centered scheme, and solved in time by an explicit second-order Runge-Kutta method.

Tab. 1 : Dynamic parameters of DNS

Grid	$(128)^3$
Box size (L)	0.128 m
Integral scale (L^E)	$1.24/1.32 \cdot 10^{-2}$ m
Reynolds number (Re_L)	39/60
Kolmogorov microscale (η)	$8.54/6.51 \cdot 10^{-4}$ s
Turbulence kinetic energy (k)	$3.22/6.53 \cdot 10^{-3} m^2 \cdot s^{-2}$
Eulerian timescale (T^E)	0.35/0.20 s
Lagrangian timescale (T^L)	0.24/0.16 s
Dispersion coefficient (D^t)	$5.1/6.8 \cdot 10^{-4} m^2 \cdot s$

Averaged equations

As shown by Overholt et al. [5], the balance equations for temperature variance and turbulence flux are written,

$$\frac{1}{2} \frac{\partial \langle \theta_f'^2 \rangle}{\partial t} = -\gamma \langle v_f' \theta_f' \rangle - \kappa_f \langle \frac{\partial \theta_f'}{\partial x_j} \frac{\partial \theta_f'}{\partial x_j} \rangle \quad (2)$$

The terms on the right hand side are production by the mean temperature gradient and dissipation due to laminar diffusivity, ϵ_θ .

$$\begin{aligned} \frac{\partial \langle \theta_f' v_f' \rangle}{\partial t} = & -\gamma \langle v_f'^2 \rangle - \langle \frac{1}{\rho_f} \theta_f' \frac{\partial p}{\partial y} \rangle \\ & - (\kappa_f + \nu_f) \langle \frac{\partial \theta_f'}{\partial x_j} \frac{\partial v_f'}{\partial x_j} \rangle \quad (3) \end{aligned}$$

The terms on the right hand side are production, pressure-scrambling and laminar dissipation.

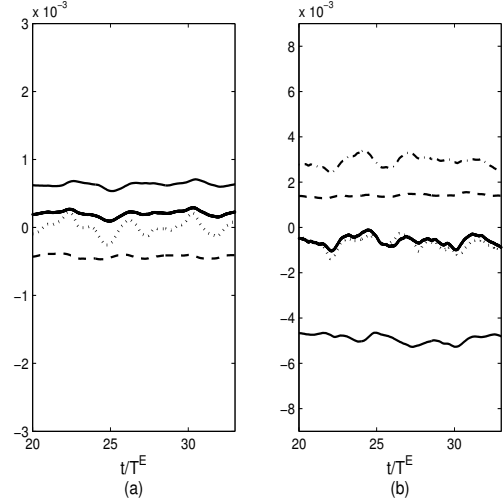


FIG. 1 Balance of variance (a) and turbulent flux (b) temperature equations : dissipation (dashed lines), production (solid lines), pressure-scrambling (dot-dashed line), time derivative (dotted lines), sum of r.h.s terms (bold lines)

Balance of the temperature correlation equations are shown by Fig. 1 for a 128^3 three-dimensional mesh. $\langle \theta_f'^2 \rangle$ and $\langle \theta_f' v_f' \rangle$ reach constant values after around four thermal Eulerian time scale T_θ^E . The measured values from the DNS can be used to calculate a thermal dispersion coefficient in the frame of gradient approximation $\langle \theta_f' v_f' \rangle = -D_\theta^t \frac{\partial \langle \theta_f \rangle}{\partial y}$. This value is reported on Table 2 and can be compared with the classical dispersion coefficient in turbulence $D^t = \frac{2}{3} k T^L$ reported on Table 1.

RESULTS AND STATISTICS

Eulerian statistics

Table 2 reports on thermal parameters and statistics from the two DNS presented in Table 1. ϵ which appears in the dissipation rate is the dynamic dissipation.

Tab. 2 : Thermal parameters of DNS

Mean temperature gradient (γ)	1
Thermal integral scale (L_θ^E)	1.26/1.35 10^{-2} m
Prandtl Number (Pr)	0.7
Temperature variance ($\theta_f'^2$)	0.34/1.32 10^{-3} K^2
Eulerian timescale (T_θ^E)	0.37/0.22 s
Lagrangian thermal timescale (T_θ^L)	0.49/0.30 s
Thermal dispersion coefficient (D_θ^t)	6.02/5.87 10^{-4} $m^2.s$
Dissipation rate (ϵ_θ/ϵ)	0.08/0.03

Next, we are presenting the two-points spatial Eulerian temperature autocorrelation functions $R_{\theta,i}^E(r) = \langle \theta_f'(\mathbf{x}, t) \theta_f'(\mathbf{x} + r\mathbf{e}_i, t) \rangle$.

Fig. 2 shows normalized auto-correlation functions $\tilde{R}_{\theta,i}^E(r)$. In the direction aligned with the mean temperature gradient, the autocorrelation function is showing a negative loop, varying with the laminar Prandtl number. In the normal directions the shape of the autocorrelation functions is very close to an exponential form.

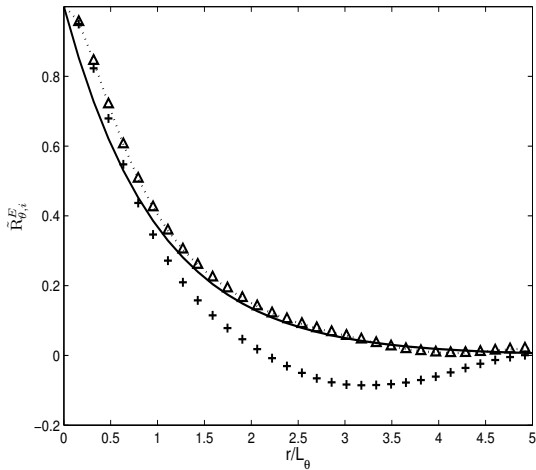


Fig. 2 Normalized spatial Eulerian autocorrelation functions in the temperature with $Pr = 0.7$. In the three directions, $i=1$ (dotted line), $i=2$ (+), $i=3$ (Δ), exponential shape (solid line). $L_\theta^E = \int_0^\infty \tilde{R}_{\theta,1}^E(r) dr$

Lagrangian statistics

Fluid velocities and temperatures predictions are interpolated on a large number (262 144) of fluid element trajectories in order to evaluate Lagrangian statistics. These interpolations are realised using a Shape Function Method [6]. Next, Lagrangian temperature autocorrelation, $R_\theta^L(\tau)$ and velocity-temperature cross-correlation, $R_{v\theta}^L(\tau)$ and $R_{\theta v}^L(\tau)$, functions are studied to characterize the temperature along the fluid element paths.

$$R_\theta^L(\tau) = \langle \theta_f'(\mathbf{x}(t), t) \theta_f'(\mathbf{x}(t + \tau), t + \tau) \rangle$$

$$R_{\theta v}^L(\tau) = \langle \theta_f'(\mathbf{x}(t), t) v_f'(\mathbf{x}(t + \tau), t + \tau) \rangle$$

$$R_{v\theta}^L(\tau) = \langle v_f'(\mathbf{x}(t), t) \theta_f'(\mathbf{x}(t + \tau), t + \tau) \rangle$$

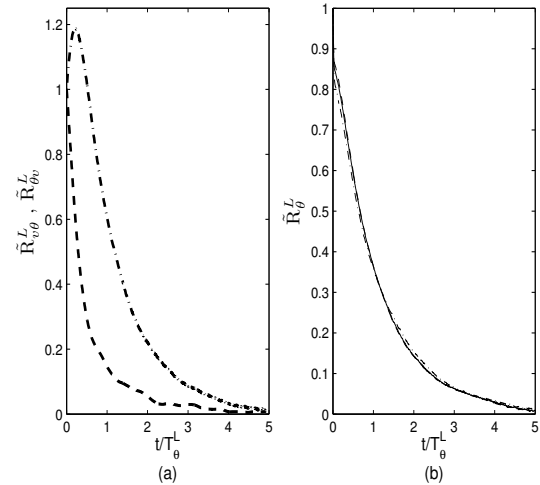


Fig. 3 Normalized Lagrangian temperature autocorrelation and velocity-temperature cross-correlation functions. (a) \tilde{R}_θ^L (dashed line) $\tilde{R}_{\theta v}^L$ (dot-dashed line) ; (b) $Pr=0.3$ (solid line), $Pr=0.7$ (dashed line), $Pr=1$ (dot-dashed line).

Lagrangian statistics are represented on Fig. 3 where laminar Prandtl numbers are smaller than unity and the value of Reynolds number (Re_{L_f}) is 39. Fig. 3 (b) presents the normalized Lagrangian temperature autocorrelation function and shows a very weak effect

of the laminar Prandtl Number. Starting from lagrangian velocity (respectively temperature) autocorrelation function, Lagrangian timescale T^L (respectively Lagrangian thermal timescale T_θ^L) could be defined by $T^L = \int_0^\infty \tilde{R}_v^L(\tau) d\tau$ and $T_\theta^L = \int_0^\infty \tilde{R}_\theta^L(\tau) d\tau$. According to the two Reynolds numbers simulated, the computed T_θ^L is around twice greater than T^L .

Normalized Lagrangian velocity-temperature cross-correlations functions are displayed on Fig. 3 (a). According to this figure, $\tilde{R}_{v\theta}^L(\tau)$ is clearly different from $\tilde{R}_{v\theta}^L(-\tau) = \tilde{R}_{\theta v}^L(\tau)$. The first function corresponds to the correlation between velocity at time t and the temperature at time $t + \tau$. During a short time interval, as shown Yeung [7], the cross-correlation increases under the coupled effect of turbulent transport and imposed mean gradient temperature in y-direction. This short time interval is close to Lagrangian timescale T^L .

LAGRANGIAN STOCHASTIC MODELS

Aiming to use a pdf approach to model heat transport in turbulent gaz-particle flows, velocity-temperature models are required. To model fluid properties along the particle path, the Langevin model approach for both velocity (4) and temperature (5) fluctuations may be used [8],

$$dv'_f = -\frac{1}{T^L} v'_f dt + B_v dW_v \quad (4)$$

$$d\theta'_f = -\frac{1}{\tau_\theta} \theta'_f dt - v'_f \gamma dt + B_\theta dW_\theta \quad (5)$$

Where dW_v and dW_θ are two independent Wiener process which have the following properties $\langle dW_v dW_v \rangle = \langle dW_\theta dW_\theta \rangle = dt$.

The model Lagrangian correlation functions can be derived from equations (4) and (5). The integration of Langevin model leads up to the analytic shape of the four correlation functions written in (6), (7), (8) and (9). So, these

model auto-correlation functions normalized by $\langle v'^2 \rangle$, $\langle \theta' v' \rangle$ or $\langle \theta'^2 \rangle$ can be compared with the ones computed from DNS as reported on Fig. 4 and Fig. 5.

$$R_v^L = \langle v'^2 \rangle e^{-t/T^L} \quad (6)$$

$$R_\theta^L = \langle \theta'^2 \rangle e^{-t/\tau_\theta} + \zeta_1 (e^{-t/T^L} - e^{-t/\tau_\theta}) \quad (7)$$

$$\text{with } \zeta_1 = \gamma \langle \theta' v' \rangle \frac{\tau_\theta T^L}{\tau_\theta - T^L}$$

$$R_{\theta v}^L = \langle \theta' v' \rangle e^{-t/T^L} \quad (8)$$

$$R_{v\theta}^L = \langle \theta' v' \rangle e^{-t/\tau_\theta} + \zeta_2 (e^{-t/T^L} - e^{-t/\tau_\theta}) \quad (9)$$

$$\text{with } \zeta_2 = \gamma \langle v'^2 \rangle \frac{\tau_\theta T^L}{\tau_\theta - T^L}$$

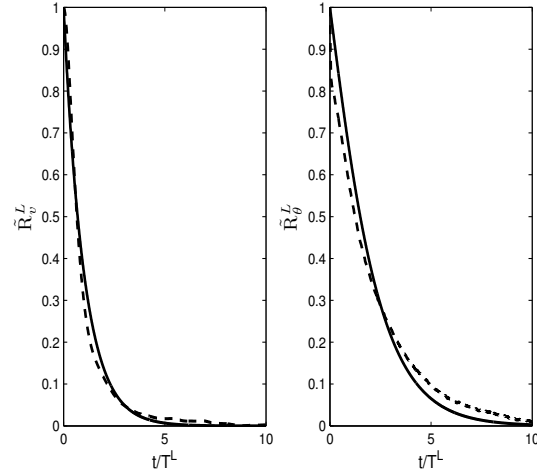


Fig. 4 Comparing of Lagrangian velocity and temperature autocorrelations from DNS (- -) with Stochastic Lagrangian model (-)

The characteristic time scale τ_θ is obtained from the definition of Lagrangian thermal timescale T_θ^L . Indeed, by integrating model Lagrangian temperature auto-correlation, τ_θ is directly obtained.

The value of τ_θ is typically about fifteen percent smaller than Lagrangian thermal timescale T_θ^L .

$$\tau_\theta = \frac{T_\theta^L}{1 - \gamma \frac{\langle \theta' v' \rangle}{\langle \theta'^2 \rangle} T_L} \quad (10)$$

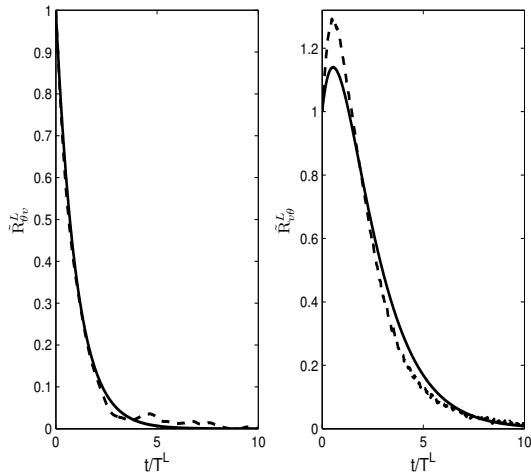


Fig. 5 Comparing of Lagrangian velocity-temperature cross-correlations computed from DNS (- -) with Stochastic Lagrangian model (-)

CONCLUSION

Direct Numerical simulations are used to characterize velocity and temperature Lagrangian statistics in non-isothermal turbulent flows. Properties of the Eulerian field are measured on a 128^3 three-dimensional mesh for two turbulent Reynolds numbers. Lagrangian auto-correlation functions computed from DNS allow to validate stochastic Lagrangian temperature model which are crucial in the development of heat transport modeling in turbulent gaz-particle flows. In addition, Lagrangian stochastic models could be validated from the moment $\langle \theta_f'^2 \rangle$ and $\langle v_f' \theta_f' \rangle$ transport equations of the joint velocity-temperature pdf using (4) and (5) closure models. The value of dispersion coefficients obtained by the moment approach could be compared with the ones of DNS.

BIBLIOGRAPHY

- [1] Simonin O., *Combustion and turbulence in two-phases flows*. In : Lecture series 1996-02. Von Karman institute for Fluid Dynamics, (1996)
- [2] Eswaran V., Pope S.B., *An examination of forcing in direct numerical simulation of turbulence*. Computers & Fluids, 316, pp. 257-278, (1988)
- [3] Fevrier P., Simonin O, Squires K.D., *Partitioning of particle velocities in gas-solid turbulent flows into a continuous and a spatially uncorrelated random distribution : theoretical formalism and numerical study*. J. Fluid Mech, 533, pp. 1-46, (2005)
- [4] Sato Y., Deutsch E., Simonin O., *Direct numerical simulations of heat transfer by solid particles suspended in homogeneous isotropic turbulence*. Int. J. heat and Fluid Flow, 19, pp 187-192, (1998)
- [5] Overholt M.R., Pope S.B., *Direct numerical simulation of passive scalar with imposed mean gradient in isotropic turbulence*. Phys. Fluids, 8, pp. 3128-3148, (1996)
- [6] Maxey M.R., *Methods for Evaluating Fluid Velocities in Spectral Simulation of Turbulence*. J. Comput. Phys., 83, pp. 96-125, (1989)
- [7] Yeung P. K., *Lagrangian characteristics of turbulence and scalar transport in direct numerical simulations*. J. Fluid Mech, 427, pp. 241-274, (2001)
- [8] Pozorski J., Waclawczyk M., Minier J-P, *Probability density function computation of heated turbulent channel flow with the bounded Langevin model*. Journal of Turbulence, 4, 011, (2003)